Monte Carlo Simulation of Star Polymer Systems with the Bond Fluctuation Model

Antonio Di Cecca and Juan J. Freire*

Departamento de Química Física, Facultad de Ciencias Químicas, Universidad Complutense, 28040 Madrid, Spain

Received September 27, 2001; Revised Manuscript Received December 10, 2001

ABSTRACT: Different systems of star polymers with 12 arms in a good solvent are investigated using a Monte Carlo algorithm with the bond fluctuation model in the dilute, semidilute, and concentrated regimes. We describe the equilibration process used for this particular type of system. Static properties of individual molecules such as the polymer sizes and asphericities are calculated. It is shown that the ratio of the star size to the size of a linear chain with the same number of units shows a noticeable variation with concentration. For dilute solutions, this ratio is in agreement with the analytical prediction for ideal star molecules. For concentrated solutions, however, it increases and approaches the simulation value for single molecules in their theta state (previously obtained with other model). Bead density profiles, together with individual and collective scattering functions, are also obtained for different concentrations, and the results are compared with predictions from the scaling theory. The impenetrability of the star cores is known to cause a discontinuity in the osmotic pressure manifested through a peak in the collective scattering functions corresponding to semidilute solutions near the overlapping concentration. We are able to detect the presence of this peak.

Introduction

The conformational properties of star polymers are significantly different from those of homologous linear chain as a result of the great influence of the central part of the star, where the density of polymer beads is very different from that in the outer parts.[1,2] This problem has been theoretically investigated with the help of scaling[3] and renormalization group[4] theories. Numerical simulation is also an alternative for exploring the features that are not fully explained by the theory or verifying the theoretical predictions. However, even though many investigations have examined the behavior of single stars, simulation studies of many-star systems are scarce, probably because of the technical difficulties entailed in equilibrating this type of polymer, for which substantial changes including the star center are difficult to accomplish. More specifically, most Monte Carlo simulations on a lattice, which are particularly efficient for the exploration of many-molecule systems,[5] have only been carried out for star solutions with three[6−8] or four[8] arms. Moreover, these simulations used the conventional simple cubic lattice, for which the implementation of adequate moves for the central unit is very complex if the number of arms is higher than four. It is clear that alternative models have to be considered for other functionalities.

The bond fluctuation model was devised to offer the computational benefit of lattice methods and the more realistic characterization of systems represented by the open-space methods in Monte Carlo simulations.[5] Perhaps the most artificial characteristics of conventional lattice methods is the choice of elementary moves for individual units. For instance, the simple cubic lattice model has to combine elementary "bents" and "crankshafts" to ensure a close-to-ergodic algorithm. For structural studies on linear chains, the use of slithering snake moves offers a more efficient alternative, although the particular disposition of elements in the lattice is still reflected in inconveniently wide regions at short distances. The problem, however, is more important if the Monte Carlo method attempts to mimic the dynamics of a polymer solution (for which elementary moves representing small random perturbations due to the thermal bath are required) or of polymers with special topologies as such stars, for which moves involving the central part are difficult to achieve. The bond fluctuation model offers a considerably higher number of empty positions available around an occupied site, and furthermore, it only needs a single and simple form of elementary move. These characteristics make this model adequate for the study of star polymers with a moderately high number of arms. However, the bond fluctuation model has been used so far only for the study of single chains and melts of three-arm stars.[9] The cooperative motion algorithm is, on the other hand, a powerful tool for equilibrating and describing structural properties of stars with high functionality in the melt state.[10]

According to the scaling theory,[3] a semidilute solution of star polymers behaves as a semidilute solution of linear chains, even though it also contains regions of starlike coronas corresponding to the star cores.[1] The crossover from the dilute to the semidilute regime occurs at the overlapping concentration, where we expect a qualitative change in the osmotic pressure. This effect corresponds to a compensation for the difference in local polymer concentration in the star core compared to the rest of the solution.[11] The osmotic pressure discontinuity leads to a peak in the scattering intensity that indicates a global ordering at the distance range equal to the mean size of a molecule. The peak is more noticeable for stars with higher numbers of arms. Our previous simulations for three or four arms with the simple cubic lattice model could only yield faint indications of this feature.

In the present work, we have performed Monte Carlo simulations of many-star systems in the dilute, semidilute, and concentrated regions. We have considered stars with 12 arms, represented by the bond fluctuation

10.1021/ma011688i CCC: $22.00
Published on Web 02/28/2002

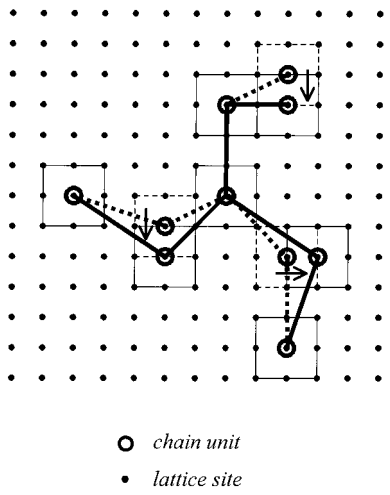

Figure 1. Bond fluctuation model for a two-dimensional star polymer. Possible moves of three monomers are indicated.

model in a simple cubic lattice. We have verified that a simple equilibration procedure leads to the expected features for equilibrated systems. We have obtained star sizes and asphericities. Moreover, we have computed the bead density profiles, the scattering functions of individual molecules (or form factors) and also the collective scattering of the systems in the different concentration regimes.

Simulation Method

In our simulations, we place n molecules, each composed of N beads divided into 12 arms and a single-bead central unit, in a cubic lattice of length L with periodic boundary conditions. The distance between adjacent sites, b, is taken as the unit of length. Each bead blocks the other 26 lattice sites contained in the elementary cube centered at the bead location. In this way, the model complies with the restrictions imposed for self-avoiding walk (SAW) polymers, and it is able to mimic the behavior of a dilute polymer molecule in a good solvent. Other additional beads (depending on the site position) can also block the 26 sites surrounding a bead. Accordingly, it is easy to verify that a single bead effectively blocks a total of eight sites. In fact, this SAW condition is completely equivalent to the description originally given for the model,[5] when "eight-site non-overlapping monomers" are substituted by single-site beads. Bonds linking the beads can have lengths ranging between 2 and $\sqrt{10}$, but bonds vectors of the type $(\pm 2, \pm 2, 0)$ are excluded to avoid bond crossing during the simulation. The value of L is chosen to be high enough to ensure that the number of interactions between different replicas of the same molecule is very small,[12] $L \geq 2N^{1/2} + 5l$, where l is the root-mean-squared bond distance ($l = 2.72$). (This condition actually gives a value of L that is considerably higher than necessary, as it was designed to comply with significantly more extended ideal linear chains.[12]) The number of molecules is determined from the desired number of sites blocked by polymer beads, which is equivalent to the polymer volume fraction $\Phi = 8nN/L^3$ (because a bead actually blocks eight box sites). Elementary bead jumps are achieved by randomly moving a bead to one of the closest six sites within its blocked cube, as shown in Figure 1. Once the move is performed, the lengths of the new bonds are checked. Also, the SAW condition is enforced by verifying that the chosen site is not blocked by any other bead. If any of these checks fails, the move is rejected. The only modification from the original model[5,13] required for the present case of 12-arm stars is that a larger area of blocked units is established around the central unit (the maximum distance between each central unit and its first neighbors increases to 4 instead of $\sqrt{10}$, as for the other beads). Only by providing this extra free space can we achieve a long-time displacement of the central units from their initial positions. Once the systems are equilibrated, the algorithm to be applied is very similar to that employed for linear chains, with the only modification being the enforcement of the bond connections of the different arms with the central unit. The general features of the code employed in the present work, therefore, were described in our recent report of simulation results for equivalent systems of linear chains.[13]

The stars are built so that they occupy regularly arranged initial positions. In the initial configuration, the arms run parallel from their second bead (neighboring the central unit) to their end, with straight bonds of $l = 2$ in a given direction, e.g., y, forming several parallel (e.g., xy) planes. These second beads are placed to comply with the model specifications using eight vectors $(\pm 2, \pm 2, \pm 1)$, two vectors $(0, \pm 3, 0)$, and two vectors $(0, 0, \pm 3)$ with origins at the central unit. The central units of different molecules are placed regularly in the system, so that a maximum number of stars (usually not more than two along the y direction) can be included within the simulation box. The minimum separation between arms of different stars must also be 2, to ensure the required minimum separation between the beads. An example of a resulting initial configuration is shown in Figure 2.

From these initial configurations, equilibration can be performed through elementary bead jumps in a reasonable amount of computing time (not significantly larger than the final run to determine properties). The typical number of Monte Carlo steps, or number of attempted elementary bead jumps divided by nN, required for the equilibration of the most concentrated systems investigated here is 10^6. The number of Monte Carlo steps used in the respective runs is 3×10^6. Only a fraction of configurations, equal to $^1/_{1000}$ of the total number of MC steps, is saved in the "trajectory files". These files contain the coordinates of the outer box that allow us to compute the different properties. In Figure 3, we show the acceptance ratio vs the number of Monte Carlo steps for a typical equilibration run. It can be observed that there is an initial decrease of the acceptance rate as the stars tend to expand in the x and z directions by "opening" their arms, because this process might involve some collisions with neighboring molecules. However, the stars simultaneously shrink in the y direction, which provides an efficient creation of free space. As a result of this effect, the acceptance rate eventually increases to reach a constant equilibration value. This value is reasonably high for all of the systems considered in the present study.

Results

(a) Mean Size and Shape and Overlapping Concentration. The mean-square radius of gyration of a molecule, $\langle S^2 \rangle$, is easily obtained from the coordinates contained in our trajectory files. The results for single-chain "dilute" systems, $\Phi \approx 0$, and for different values

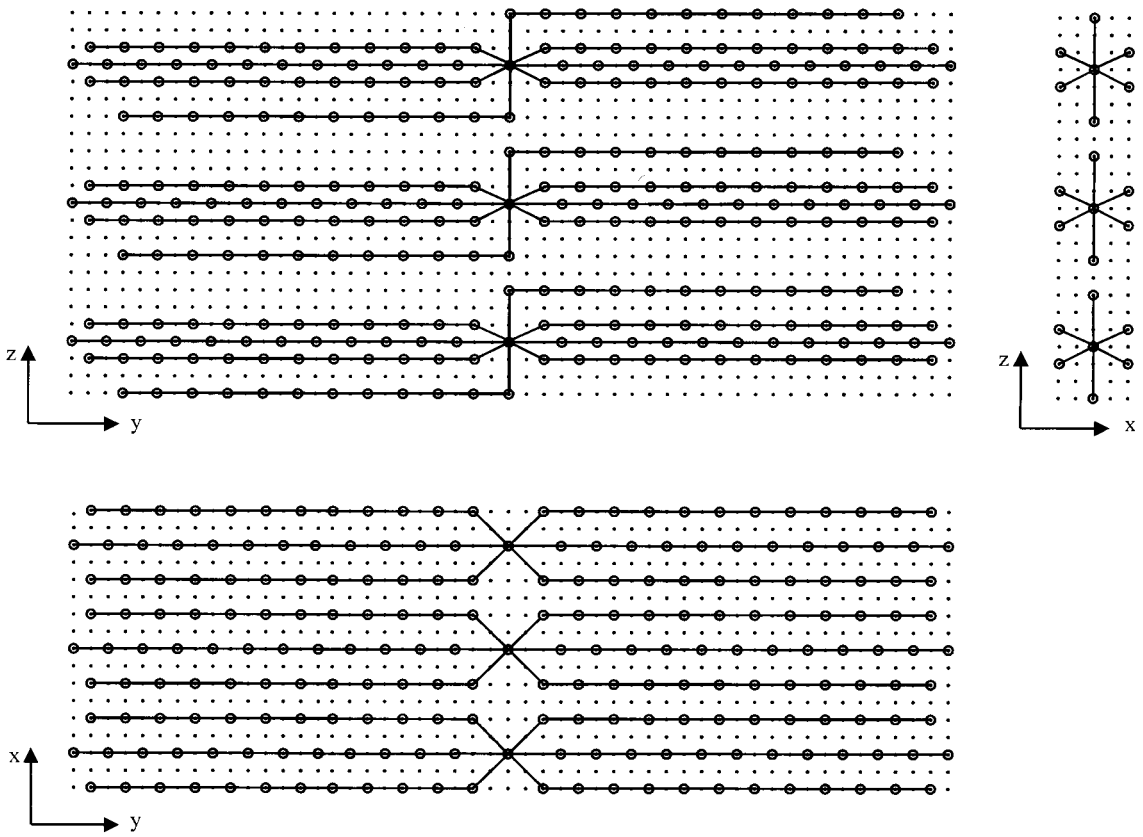

Figure 2. Initial configuration for bond fluctuation model star chains with 12 arms and $N = 145$ in a cubic lattice. Only part of the box size is shown in the three projections.

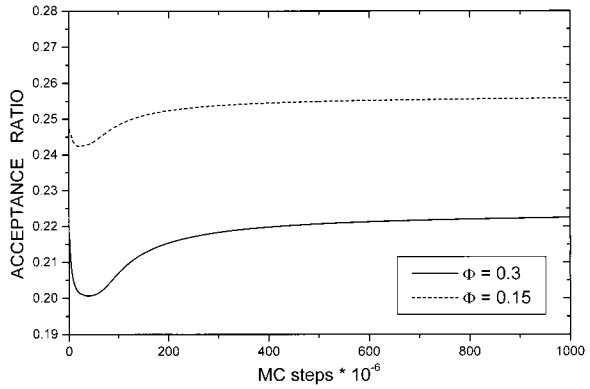

Figure 3. Acceptance ratio vs number of MC steps for the equilibration of a chain with $N = 145$ at different concentrations.

of Φ are given in Table 1. According to the scaling theory,[3] the size of a single star immersed in a good solvent (excluded-volume conditions) scales with the total number of units N similarly to a linear chain, i.e., we can write

$$\langle S^2 \rangle^{1/2} \approx N^{\nu} \qquad (1)$$

where ν is a critical exponent whose value has been calculated[14] to be $\nu = 0.588$. Values of ν, considered as a parameter fitted from linear representations of $\log\langle S^2 \rangle$ vs $\log N$, are contained in Table 1. The result obtained from dilute systems is very close to the critical exponent. However, we should take into account some subtle features to fully understand this coincidence. Our similar study of linear chains[13] with the same model

Table 1. Size- and Shape-Related Quantities Obtained for Different Concentrations and Different Values of *N*

Φ	N	$\langle S^2 \rangle$	g	$\langle R_{ce}^2 \rangle$	$\langle R_{ce}^2 \rangle / \langle S^2 \rangle$	$\langle A \rangle$	ν^a
0.3	289	160.61	–	305.96	1.90	0.0706	
0.3	145	83.34	0.294	153.91	1.85	0.0630	
0.3	109	64.77	0.311	117.83	1.82	0.0584	
0.3	73	44.08	0.326	77.90	1.77	0.0534	
0.3							0.469
0.15	289	197.61	–	377.35	1.91	0.0637	
0.15	145	98.71	0.291	184.91	1.87	0.0550	
0.15	109	74.60	0.302	138.44	1.85	0.0517	
0.15	73	49.13	0.310	88.37	1.80	0.0478	
0.15							0.505
0.075	289	229.93	–	447.20	1.94	0.0599	
0.075	145	108.05	0.277	205.73	1.90	0.0510	
0.075	109	79.14	0.282	148.59	1.88	0.0486	
0.075	73	51.12	0.288	92.83	1.82	0.0457	
0.075							0.546
0.04	289	244.14	–	478.45	1.96	0.0553	–
0.0	289	255.72	–	502.98	1.97	0.0530	
0.0	145	113.17	0.236	219.31	1.94	0.0496	
0.0	109	81.45	0.241	152.97	1.88	0.0484	
0.0	73	51.79	0.251	94.30	1.82	0.0460	
0.0							0.581

[a] Values of ν are calculated from a log−log linear fit of $\langle S^2 \rangle$ vs N.

for a range of values of units, $N \leq 100$ (similar to the present values of N/f) yields $\nu = 0.62$ for the single-chain systems. This result is slightly but noticeably higher than the theoretical prediction and is explained by a quantitative analysis of finite-size effects. The smaller value of ν obtained here should, therefore, interpreted as the consequence of further finite-size effects due to the presence of the star core. These additional core effects tend to decrease the ν values of finite star chains

with respect to those of linear chains of similar extension. Therefore, the excellent agreement of our value of ν for dilute systems of 12-arm stars with the theory might be due to the cancellation of opposite finite-size effects.

The ratio, g, of the size of a branched chain (or star) to that of a linear chain with the same number of units (or molecular weight), i.e.

$$g = \langle S^2 \rangle_{br} / \langle S^2 \rangle_{lin} \tag{2}$$

can be used to characterize the branching architecture.[1,2,4] Applying Gaussian statistics for intramolecular distances between units, i.e., ignoring excluded-volume or any other type of long-range intramolecular interactions, an analytical formula for the ratio g for long ideal molecules has been derived as

$$g = (3f - 2)/f^2 \tag{3}$$

The application of the renormalization group shows that eq 3 also gives a good estimation of g for polymers under excluded-volume conditions,[4] i.e., for dilute polymers in a good solvent. This conclusion has been verified through experimental measurements and single-molecule numerical simulations.[1,2,4] In Table 1, we also include results for g. These values were obtained by combining the present results for the radius of gyration of 12-arm stars with estimations of their homologous values for linear chains. The latter estimations are based on our previous study of linear chains with the same model and concentrations.[13] (The results for $\langle S^2 \rangle$ at different chain lengths provide a fit to eq 1, from which we can compute $\langle S^2 \rangle$ for linear chains at the values of N that correspond to our 12-arm stars.) It is verified that our results for dilute systems are in good agreement with the $g = 0.236$ prediction of eq 3 for $f = 12$, and this agreement is remarkable for high N. We should mention at this point that g is greater for single molecules at the theta point. In this case, neither a linear chain nor the most external part of a star is perturbed, and therefore, both behave ideally. However, the influence of three-body effects in the core causes an expansion of the arms within this region. Then, the ratio g for dilute molecules in the theta state is greater than that for ideal polymers.[1,2,4] An apparently accurate estimation for 12-arm stars at the theta point, based in simulation results obtained with relatively high values of N, is $g = 0.28$.[15]

Also, we show in Table 1 the results computed for the mean-square center-to-end distance of individual arms, $\langle R_{ce}^2 \rangle$. The value of the ratio $\langle R_{ce}^2 \rangle / \langle S^2 \rangle$ should be considerable smaller than the result for a linear chain. For ideal linear chains, $\langle R_{ce}^2 \rangle = \langle R^2 \rangle / 2$, where $\langle R^2 \rangle$ is the mean-square end-to-end distance. Also, for ideal linear chains, we have $\langle R^2 \rangle = Nl^2$ and $\langle S^2 \rangle = Nl^2/6$. Therefore, we can write $\langle R_{ce}^2 \rangle / \langle S^2 \rangle = 3$ as an estimation for the upper limit of this ratio. Moreover, taking into account eqs 2 and 3 for an ideal star of f arms, together with $\langle R_{ce}^2 \rangle = (N/f)l^2$, we obtain $\langle R_{ce}^2 \rangle / \langle S^2 \rangle = 6f/(3f - 2)$, i.e., $\langle R_{ce}^2 \rangle / \langle S^2 \rangle = 2.118$ for the 12-arm stars. Another reference is the result for a compact sphere of radius R_{ce}, for which $R_{ce}^2/S^2 = {}^5/_3$. All of the results for $\langle R_{ce}^2 \rangle / \langle S^2 \rangle$ in Table 1 are bracketed by the two latter values, with a closer approach to the compact sphere for the stars with fewer units (or a relatively more extended core). The data show a very noticeable variation with N. Fitting the results of the ratio corresponding to the dilute systems vs $1/N^{1/2}$, we obtain a long-chain extrapolated limit of 2.14. This result is very close to the prediction for ideal molecules, although slightly higher. A possible explanation of this apparently ideal behavior is that excluded-volume interactions are partially or totally canceled in these ratios, as happens in the more widely investigated case of ratio g.

As an indication of the average shape of individual molecules, we also computed the asphericity

$$\langle A \rangle = \frac{\langle \sum_i^3 \sum_j^3 (\lambda_i - \lambda_j)^2 \rangle}{4 \langle (\sum_i^3 \lambda_i)^2 \rangle} \tag{4}$$

where the eigenvalues λ_k are obtained through the numerical diagonalization of the 3×3 tensor of quadratic components of the radius of gyration of individual molecules in each configuration. The computed results for $\langle A \rangle$ are also included in Table 1. Our results for dilute stars are slightly smaller than the theoretical prediction for ideal polymers[16]

$$\langle A \rangle = \frac{10(15 - 14/f)/f}{15(3 - 2/f)^2 + 4(15 - 14/f)/f} \tag{5}$$

$\langle A \rangle = 0.0922$ for $f = 12$. The presence of excluded-volume effects seem to favor a smaller $\langle A \rangle$, i.e., more spherical shapes, for the stars, a result opposite to the trend observed for linear chains.[2] As the chain length increases, our results tend to agree with the asymptotic value $\langle A \rangle = 0.0558$ obtained for very long SAW molecules with a different lattice model.[17]

It is well-known that the excluded-volume effects are screened out for chains in melts or concentrated solutions.[14] The dilute regime is delimited by the concentration at which molecules start to overlap. This critical concentration, Φ^* in volume fraction, is easily estimated for linear chains as the value that equals the mean density of beads inside a molecules. The chain volume is estimated from the value of $\langle S^2 \rangle$ in dilute solution, $\langle S^2 \rangle_0$, and, therefore

$$\Phi^* = aN/(4\pi \langle S^2 \rangle_0^{3/2}/3) \tag{6}$$

with $a \approx 1$. Actually, the internal density of beads is not constant within a polymer coil, being always smaller at its external part. However, this effect is not particularly relevant for linear chains. In the case of star polymers, however, the bead density at the star core is similar to that in the melt state, and the internal density of beads decreases substantially from the core to the external region. This change in density is described as a function from the star center, $\rho(r)$, by the scaling theory for stars of high functionality,[3] which predicts

$$\rho(r) = Cr^{(1-3\nu)/\nu} \tag{7}$$

where C is a numerical constant. These predictions for bead density profiles $\rho(r)$ have been extensively verified in the past through numerical simulations[1] for single stars. Therefore, because the actual density in the external part of a star that overlaps with other mol-

Table 2. Overlapping Concentrations Φ* for Different Chain Lengths Calculated from Equation 6 with $a = 0.2$ and the Radius of Gyration for Dilute Solutions

$(N-1)/f$ [a]	N	Φ*
6	73	0.0748
9	109	0.0566
12	145	0.0460
24	289	0.0270
48	577	0.0162

[a] In the first column, the number of units for each arm is shown.

ecules is much smaller than the density in the core, eq 6 (which is based on a mean value) gives an important overestimation of the actual value of Φ*. We have introduced this feature by interpreting a in eq 6 as a numerical constant smaller than 1 for stars with enough arms to follow the scaling theory. a is derived by assuming that the external region of the star is described by the value r_{ext}, which we set as the upper limit of r in the integration of the radial density over the star volume. This integration should provide the total number of units in the star N

$$\int_0^{r_{ext}} \rho(r)(4\pi r^2)\, dr = N \tag{8}$$

This is consistent with assuming that $\rho(r) = 0$ for $r > r_{ext}$. To perform this integration, we assume that the form of $\rho(r)$ is given by eq 7. Equation 8 provides the proportionality constant C in eq 7 in terms of r_{ext} and N. According to the scaling theory,[1,3] C and, therefore, r_{ext} depend on the number of arms. Once C is known, it is possible to obtain the mean density within the bead $\langle\rho(r)\rangle$ also in terms of r_{ext} and N as

$$\langle\rho(r)\rangle = \int_0^{r_{ext}} \rho^2(r)(4\pi r^2)\, dr/N \tag{9}$$

Following these specifications, the ratio between the external and mean densities in a many-arm star is obtained as a numerical value that can be identified with the correction constant a in eq 6. With $\nu \approx {}^3/_5$, we obtain the result

$$a = \rho(r_{ext})/\langle\rho(r)\rangle \approx {}^1/_5 \tag{10}$$

which does not depend on f. Numerical results for the overlapping concentrations obtained from eq 6 with this value of a are shown in Table 2.

Table 1 also contains simulation results for nondilute systems. Actually, the nondilute regime expands to all of our systems with $\Phi \neq 0$, because, for 12-arms stars, eq 6 with $a = {}^1/_5$ yields $\Phi^* \approx 0.075$ for $N = 73$ and $\Phi^* \approx 0.03$ for $N = 289$, where we include a simulation with $\Phi^* = 0.04$ (see Table 2). The nondilute results in Table 1 clearly show effects due of the excluded-volume screening. Thus, the fitted exponents ν are smaller than the critical value, and they even become smaller than the ideal-chain result $\nu = 0.5$ as the concentration increases. However, this further decrease of ν from the theoretical prediction is not an indication that the molecule tends to collapse; rather, it simply reflects the same finite-size effects due to the presence of a large and compact core in these less extended molecules, which we have previously discussed for the dilute systems.

The screening of excluded-volume effects also explains the increase of the asphericity with the concentration. At high values of Φ, the results are closer to the theoretical limit for ideal chains given by eq 5, noticeably departing from the excluded-volume values obtained for the dilute systems.

It is very interesting to note that, for long chains at the highest concentrations, we obtain values of g very close to the estimation from single-molecule simulations at the theta point,[15] deviating from the dilute-regime, or excluded-volume, values, which can adequately be described by eq 3 for ideal chains. Therefore, we should conclude that the core effects cause a noticeable increase of g with concentration. Our previous simulations[8] for $f = 3$ and 4 with the simple cubic lattice model indicated, however, an almost constant value of g close to the prediction for ideal star molecules at different concentrations. Of course, core effects are not as significant in the case of stars with small numbers of arms.

The ratio $\langle R_{ce}^2\rangle/\langle S^2\rangle$ for the same N in Table 1 is slightly smaller at higher concentrations. This is another, although fainter, indication of the screening of excluded volume that leads to a higher density of beads in the external region of the stars, giving results closer to the compact-sphere limit. However, the main variation of these ratios is with N, because, as already discussed for the dilute systems, the data are significantly affected by finite-size effects. A fit of the results for $\Phi = 0.3$ vs $1/N^{1/2}$ leads to the extrapolated value $\langle R_{ce}^2\rangle/\langle S^2\rangle = 2.04$, which is actually smaller than the theoretical prediction for ideal chains. This discrepancy might be due to the absence of intermolecular interactions in the internal region. Therefore, the expansion of the arms inside the core cannot be screened out, and this expansion makes an important contribution in $\langle S^2\rangle$. On the other hand, although $\langle R_{ce}^2\rangle$ describes a similar core expansion in two arms, these arms can extend significantly to the outside region of the main star volume, where the expansion effects are more effectively canceled by the presence of other chains. Consequently, $\langle R_{ce}^2\rangle$ makes a larger contribution of the nonexpanded part of the star.

(b) Bead Density Profiles and Scattering Functions. We also obtained bead density profiles $\rho(r)$ by computing the mean density of beads at different values of the radial coordinate r from the centers of individual molecules in the system. For many-molecule systems, we distinguish between the intramolecular bead density, $\rho_{int}(r)$, for which we only take into account the bead belonging to the molecule whose center is used for reference, and the total bead density $\rho(r)$. $\rho_{ext}(r) = \rho(r) - \rho_{int}(r)$ gives the intermolecular profile, i.e., the density of beads belonging to other molecules at a given distance from the center of particular star.

Figure 4 shows the results corresponding to these three different types of profiles for a star with $N = 289$ at $\Phi = 0.04$ The aspects of the initial parts of $\rho(r)$ and $\rho_{int}(r)$ are very similar as beads from other molecules are unlikely to penetrate the region near the compact star core. Log−log fits of these initial parts give slopes close to the theoretical exponent $(1 - 3\nu)/\nu$ in eq 7, $(1 - 3\nu)/\nu = -{}^4/_3$ for $\nu = {}^3/_5$. The investigation of these slopes for long single-star molecules with different models and simulation techniques has been extensively accomplished in the past,[1] confirming the predictions from the scaling theory.

The nonzero intermolecular and total profiles at large r initially reflect the interpenetration of the external parts of the stars. In Figure 4, it is observed that, at

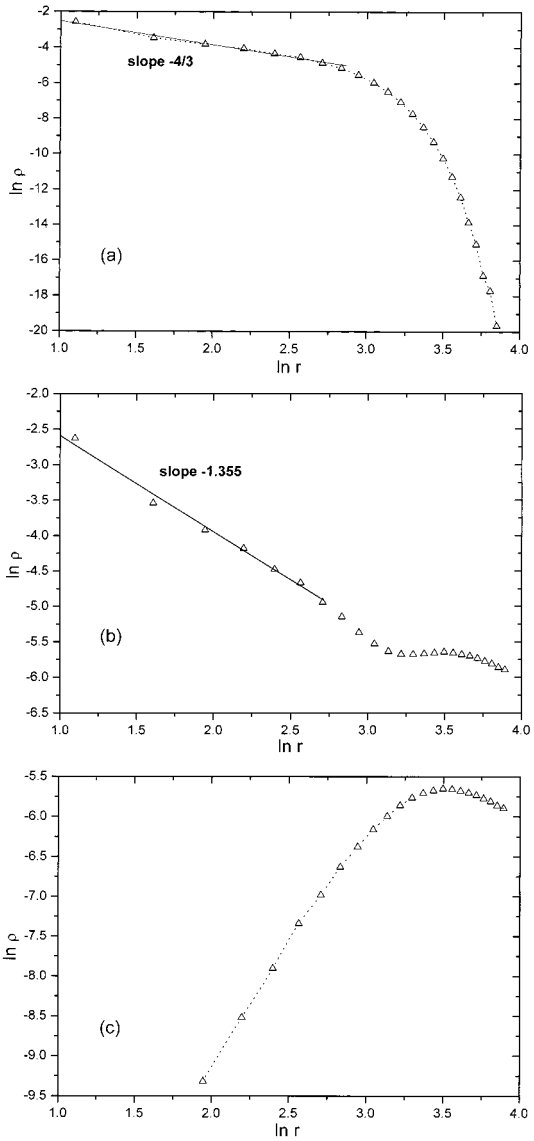

Figure 4. Bead density profiles for star chains with $N = 289$ at $\Phi = 0.04$: (a) intramolecular bead density, (b) total bead density, (c) intermolecular bead density. Fitted initial slopes are indicated as solid lines.

sufficiently high values of r, these densities exhibit a wide peak. The peak reflects the presence of the cores of other stars, which are disposed to forming an ordered structure across the system volume. The intermolecular profiles decrease at even higher values of r, and as a result of limitations due to the finite box size, we have not been able to reach the region of values of r for which the density reaches its lowest plateau value for this particular concentration.

A different and more global view of the bead distribution is achieved from the computation of scattering functions, as they contain contributions both from the mean density profile and also from density fluctuations.[18] The collective scattering function is computed as

$$S(q) = 8L^{-3}\langle[\sum_i^{L^3} f_i \cos(\mathbf{q}\cdot\mathbf{R}_i)]^2 + [\sum_i^{L^3} f_i \sin(\mathbf{q}\cdot\mathbf{R}_i)]^2\rangle \quad (11)$$

where f_i is the occupation state of the different sites, located at $\mathbf{R}_i$, within the simulation box lattice and is given by

$$f_i = 1 - \Phi/8 \quad (12a)$$

if site i contains a bead unit or

$$f_i = -\Phi/8 \quad (12b)$$

if site i is blocked or empty, to comply with the requirement that the global system considered as a single macroscopic volume does not scatter. (The factors reduce to 1 or 0 for occupied and unoccupied sites, respectively, for dilute solutions.) In this assignment of contrast factors, we have considered that the additional seven sites effectively blocked by any chain bead are "solvent sites". (We cannot easily assign these blocked sites as "polymer beads" as a site can be actually blocked by a changing number of monomer beads.) This strategy implies an average contrast factor of $(1 - \Phi)$ for the scattering volume of the eight blocked sites associated with each bead. With the introduction of the factor 8 in eq 11, the results should be equivalent to those obtained with contrast factors of $(1 - \Phi)$ for each blocked site and $-\Phi$ for each nonblocked solvent site, i.e., when the total scattering per volume unit is 8 times higher. The latter assignment is easy to perform in the conventional simple cubic lattice model[8] or in the original description of the bond fluctuation model.[5] With these specifications, the practical distinction between a single bead surrounded by seven "blocked solvent sites" (in our description) and "eight-site monomers" (in the original description) would only be relevant for values of $q \equiv |\mathbf{q}|$ high enough to monitor regions smaller than b.

To compute $S(q)$, we have to comply with the following restrictions, imposed on q by the periodic boundary conditions according to the chosen box length

$$q_k = (2\pi/L)n_k, \quad k \equiv x, y, z; \quad n_k = 1, 2, \ldots \quad (13)$$

We also define the form factor of individual molecules as

$$P(q) = N^{-2}\langle[\sum_i^N \cos(\mathbf{q}\cdot\mathbf{R}_i)]^2 + [\sum_i^N \sin(\mathbf{q}\cdot\mathbf{R}_i)]^2\rangle \quad (14)$$

where $\mathbf{R}_i$ now denotes the position of bead i inside a molecule calculated directly from the coordinates of the outer box using an internal reference. For single-molecule systems, $S(q) \approx N\Phi P(q)$.

Sometimes, it is convenient to analyze scattering functions in terms of the scaled variable x

$$x = q^2\langle S^2\rangle \quad (15)$$

In Figure 5, we show the values of $P(x)$ obtained for star chains with $N = 289$ in the dilute and nondilute regimes. At small x, we can observe the behavior in the Guinier regime, for which the molecule is considered as a whole. We can observe that the scaled form factors do not depend on concentration. All of the values in this regime are adequately described by a theoretical expression for ideal star chains in terms of x and f that was derived some time ago by Benoit,[19] which is also represented. Higher values of x correspond to the blob regime, where we observe the individual scattering of internal parts of the chain, or blobs, whose sizes are proportional to $1/q$, immersed in the solvent. Similarly

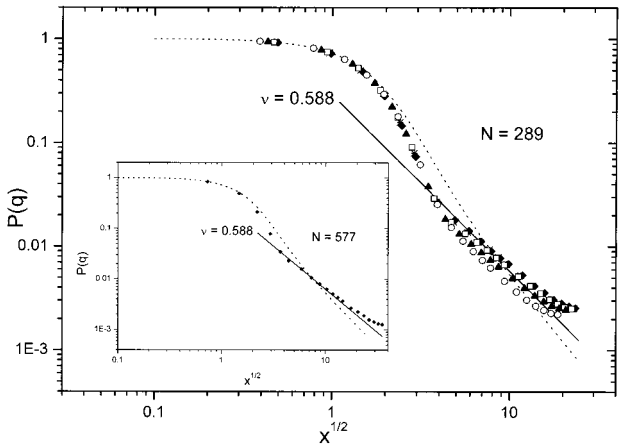

Figure 5. Log−log plot of the scattering form factor vs $x^{1/2}$ for star chains with $N = 289$ at different concentrations (◆, $\Phi = 0$; ∗, $\Phi = 0.040$; □, $\Phi = 0.075$; ▲, $\Phi = 0.15$; ○, $\Phi = 0.3$). The scattering form factor, for a star chain with $N = 577$ at $\Phi = 0$, is shown in the inset. The dashed lines correspond to the Benoit function for an ideal uniform star chain.[2] The solid lines indicate the slope corresponding to the blob regime.

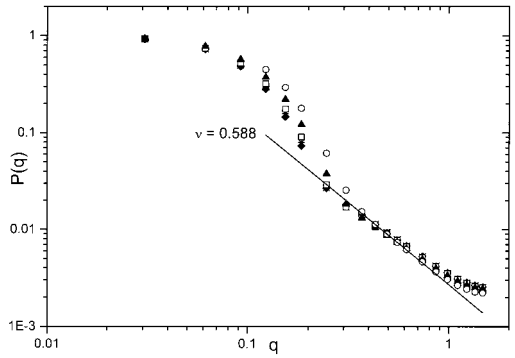

Figure 6. Log−log plot of the scattering form factor vs q for star chains with $N = 289$ at different concentrations. See Figure 5 for notation.

to the scaling law for the whole molecule (eq 1), the blob size, ξ, depends on the number of units that it contains, n_b, as $\xi \approx n_b^{\nu}$. Therefore, the scattering is proportional to the number of units monitored; we expect that, in this regime

$$P(q) \approx q^{-1/\nu} \tag{16}$$

In Figure 5, we verify that the blob regime is restricted to a relatively narrow range of x. In the inset, we can observe how the range of values of x in the blob regime extends further in a larger star with $N = 577$. The different systems show a universal behavior in the blob regime when we consider a representation in terms of the q variable, as can be seen in Figure 6. (The differences observed in Figure 5 for different concentrations correspond to the previously discussed variation of the chain size with Φ.) For higher values of q, all of the data are still grouped, but they deviate upward, reflecting model-dependent details of local regions containing a few beads.

In Figure 7, we show our simulation values of the collective scattering function for a star with $N = 145$ at different concentrations. As in the case of the form factors, we can distinguish different behaviors at different q ranges. In the small-q range, the nondiluted systems do not follow the Guinier regime as the chains

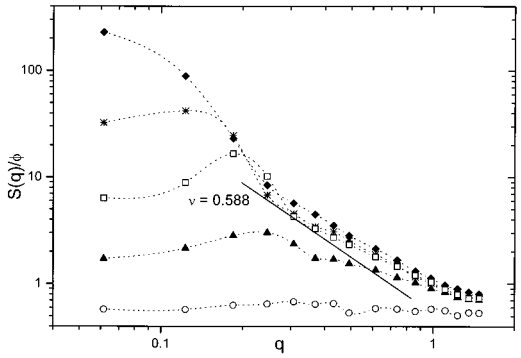

Figure 7. Normalized collective scattering function vs q obtained for $N = 289$ at different concentrations (◆, $\Phi = 0$; ∗, $\Phi = 0.040$; □, $\Phi = 0.075$; ▲, $\Phi = 0.15$; ○, $\Phi = 0.3$). The solid line indicates the slope corresponding to the blob regime.

overlap. The results in this regime can be obtained in terms of the osmotic compressibility as[20]

$$S(q\rightarrow 0) \approx \Phi(\partial\pi/\partial\Phi)^{-1} \tag{17}$$

which, together with the result for semidilute solutions[14]

$$\pi \approx \Phi^{1+1/(3\nu-1)} \tag{18}$$

gives

$$S(q\rightarrow 0)/\Phi \approx \Phi^{-1/(3\nu-1)} \tag{19}$$

$S(q\rightarrow 0)/\Phi$ can be estimated from the apparent low-x plateau in each of the three intermediate semidilute scattering functions represented in Figure 7. We have included these three data vs Φ in a log−log linear fit, obtaining a value of -2.21 for the exponent in eq 19, with a good correlation. Although the qualitative decrease of $S(q\rightarrow 0)$ with Φ is confirmed, this result differs from the exponent $-5/4$ obtained from eq 19 with $\nu = 3/5$, being, in fact, consistent with a smaller value of ν. Perhaps the extra increase of the osmotic pressure due to the impenetrability of the cores can explain the more negative exponent resulting from our fit, as the theoretical scaling law for the variation of this property with concentration shown in eq 18 was actually derived for linear chains.

The impenetrability and ordered disposition of the cores are features clearly associated with the peaks that we observe in some of the nondilute systems at intermediate values of q. The peaks are explained as being due to a discontinuity in the osmotic pressure at the overlapping concentration,[21] and in fact, they are more prominent for the concentrations closest to Φ^*. The maximum appear at higher q as the concentration increases, because the stars tend to penetrate each other further at higher concentrations, which allows the cores to become closer. The same types of peaks have also been detected in neutron scattering experiments,[22,23] and they have also been shown in recent theoretical calculations for structure factors.[24] The dependence of the intensity and location of the experimental peaks on concentration is in agreement with the simulation results. The experimental peaks become very pronounced for stars with high numbers of arms, also in agreement with scaling theory.[21] In previous simulations with the simple cubic lattice, we were able to detect some roughness in the collective scattering function at intermediate q, which can be a subtle signature

of this feature for stars with three and four arms. An additional difficulty in detecting the peaks in these latter systems is that the considered concentrations were significantly higher than Φ^*. (The overlapping concentrations given in ref 8 were probably overestimated, as they were calculated from eq 6 with $a = 1$ and some core effect corrections might be needed even for stars with small numbers of arms.)

We can also observe in Figure 7 that all of the results for $\Phi \approx 0$, $\Phi = 0.04$, and $\Phi = 0.075$ tend to converge at high values of q beyond the peak maximum. These results for different concentrations are compatible with the blob regime. The existence of a blob regime in a nondilute system shows that this system is in the semidilute region. However, the precise agreement with the blob regime and the universal dependence on q shown by the form factors are somehow affected by the nearby presence of the peaks in the present case of collective scattering. The data for $\Phi = 0.15$ apparently follow a similar trend, although, in this case, the peak distorts the characterization of the blob regime to a much greater extent. At higher values of x, the data for these three concentrations are even closer, but the curves abandon the blob regime to reflect local model-dependent details. The $\Phi = 0.3$ scattering curve, however, is rather flat, only showing a faint roughness at values of q compatible with the peak location. Therefore, this scattering curve corresponds to a solution in the concentrated regime that cannot exhibit the blob regime, although it must eventually merge with the curves corresponding to the rest of the systems at very high values of q.

Concluding Remarks

The ratio of the star size to the size of a linear chain, both in a good solvent, varies with concentration. For dilute solutions, this ratio is in agreement with the analytical prediction for ideal star molecules. For concentrated solutions, it increases, approaching previous simulation results obtained for dilute solutions in the theta state. Also, the asphericity values tend to agree similarly with the ideal and theta single-chain results for dilute and concentrated solutions, respectively. The collective scattering functions tend to agree with the expected behavior of individual blobs at high q, as predicted by the scaling theory. This behavior is also reflected in the low-r behavior of the intramolecular and total bead profiles. Compared with the theoretical prediction of the scaling theory for linear chains, the collective scattering functions at low q in the semidilute regime show a further decrease with concentration. The intermolecular and total bead profiles suggest some degree of ordering in the nondilute solutions. This ordering is confirmed through the appearance of a peak in the collective scattering functions corresponding to semidilute solutions near the overlapping concentration. This peak has been previously found in experiments. According to theory, the peak is due to the impenetrability of the star cores, which causes a discontinuity in the osmotic pressure. Therefore, the present simulations are able to capture the most relevant physical features of nondilute solutions of star chains with sufficient numbers of arms to exhibit core effects.

Acknowledgment. This work was supported by the European TMR Research Network "NEWRUP" and Grant PB98-0791 of the DGICYT (MEC, Spain). We acknowledge useful discussions with Prof. J. S. Pedersen, Risø National Laboratory, Roskilde, Denmark.

References and Notes

(1) Grest, G. S.; Fetters, L. J.; Huang, J. S.; Richter, D. *Adv. Chem. Phys.* **1996**, *94*, 67.
(2) Freire, J. J. *Adv. Polym. Sci.* **1999**, *143*, 35.
(3) Daoud, M.; Cotton, J. P. *J. Phys.* **1982**, *43*, 531.
(4) Douglas, J. F.; Roovers, J.; Freed, K. F. *Macromolecules* **1990**, *23*, 4168.
(5) Binder, K. In *Monte Carlo and Molecular Dynamics Simulations in Polymers*; Binder, K., Ed.; Oxford University Press: New York, 1995.
(6) Sikorsky, A. *Makromol. Chem. Theory Simul.* **1993**, *2*, 309.
(7) Sikorski, A.; Romiszowski, P. *J. Chem. Phys.* **1996**, *104*, 8703.
(8) Molina, L. A.; Freire, J. J. *Macromolecules* **1999**, *32*, 499.
(9) Brown, S.; Szamel, G. *Macromol. Theory Simul.* **2000**, *9*, 14.
(10) Pakula, T.; Vlassopoulos, D.; Fytas, G.; Roovers, J. *Macromolecules* **1998**, *31*, 8931.
(11) Witten T. A.; Pincus P. *Macromolecules* **1986**, *19*, 2509.
(12) Kremer, K. *Macromolecules* **1983**, *16*, 1632.
(13) Rubio, A. M.; Storey, M., Lodge; J. F. M.; Freire, J. J. *Macromol. Theory Simul.* **2002**, *11*, 171.
(14) de Gennes, P.-G. *Scaling Concepts in Polymer Physics*; Cornell University Press: Ithaca, NY, 1979.
(15) Batoulis J.; Kremer, K. *Europhys. Lett.* **1989**, *22*, 4277.
(16) Wei, G.; Eichinger, B. E. *J. Chem. Phys.* **1990**, *93*, 1430.
(17) Zifferer, G. *Macromol. Chem.* **1991**, *192*, 1555.
(18) Auvray, L.; de Gennes, P.-G. *Europhys. Lett.* **1986**, *2*, 647.
(19) Benoit, H. *J. Polym. Sci.* **1953**, *11*, 507.
(20) des Cloizeaux, J.; Jannick, G. *Polymers in Solution*; Clarendon Press: Oxford, U.K., 1990.
(21) Witten, T. A.; Pincus, P. A.; Cates, M. E. *Europhys. Lett.* **1986**, *2*, 137.
(22) Richter, D.; Jucknischke, O.; Willner, L.; Fetters, L. J., Lin, M.; Huang, J. S.; Roovers, J.; Toporowski, P. M.; Zhou, L. L. *J. Phys. IV Suppl.* **1993**, *3*, 3.
(23) Marques, C. M.; Izzo, D.; Charitat T.; Mendes, E. *Eur. Phys. J. B* **1998**, *3*, 353.
(24) Pedersen, J. S. *J. Chem. Phys.* **2001**, *114*, 2839.

MA011688I